

# Fine-tuning Diffusion Models for Enhancing Face Quality in Text-to-image Generation

Zhenyi Liao<sup>1</sup>, Qingsong Xie<sup>2\*</sup>, Chen Chen<sup>2</sup>, Haonan Lu<sup>2</sup>, and Zhijie Deng<sup>1\*</sup>

<sup>1</sup> Qing Yuan Research Institute, SEIEE, Shanghai Jiao Tong University

<sup>2</sup> OPPO AI Center

l-justice@sjtu.edu.cn, {xieqingsong1, chenchen4, luhaonan}@oppo.com,  
zhijied@sjtu.edu.cn

**Abstract.** Diffusion models (DMs) have achieved significant success in generating imaginative images given textual descriptions. However, they are likely to fall short when it comes to real-life scenarios with intricate details. The low-quality, unrealistic human faces in text-to-image generation are one of the most prominent issues, hindering the wide application of DMs in practice. Targeting addressing such an issue, we first assess the face quality of generations from popular pre-trained DMs with the aid of human annotators and then evaluate the alignment between existing metrics such as ImageReward [48], Human Preference Score [47], Aesthetic Score Predictor [8], and Face Quality Assessment [27], with human judgments. Observing that existing metrics can be unsatisfactory for quantifying face quality, we develop a novel metric named *Face Score (FS)* by fine-tuning ImageReward on a dataset of (good, bad) face pairs cheaply crafted by an inpainting pipeline of DMs. Extensive studies reveal that *FS* enjoys a superior alignment with humans. On the other hand, *FS* opens up the door for refining DMs for better face generation. To achieve this, we incorporate a guidance loss on the denoising trajectories of the aforementioned face pairs for fine-tuning pre-trained DMs such as Stable Diffusion V1.5 [35] and Realistic Vision V5.1 [40]. Intuitively, such a loss pushes the trajectory of bad faces toward that of good ones. Comprehensive experiments verify the efficacy of our approach for improving face quality while preserving general capability. We will release source codes and datasets upon acceptance of the paper.

**Keywords:** Diffusion models · Text-to-image generation · Face quality

## 1 Introduction

Diffusion models (DMs) [16, 29, 44] have emerged as a prominent type of generative models, finding applications in various generative tasks such as audio generation [7, 20], video generation [4, 14, 15], and image inpainting [1, 2, 25]. Among these tasks, text-to-image DMs, such as Stable Diffusion (SD) [31, 35], Midjourney [26], and others [28, 34, 38], have garnered significant attention and

---

\*Corresponding authors.

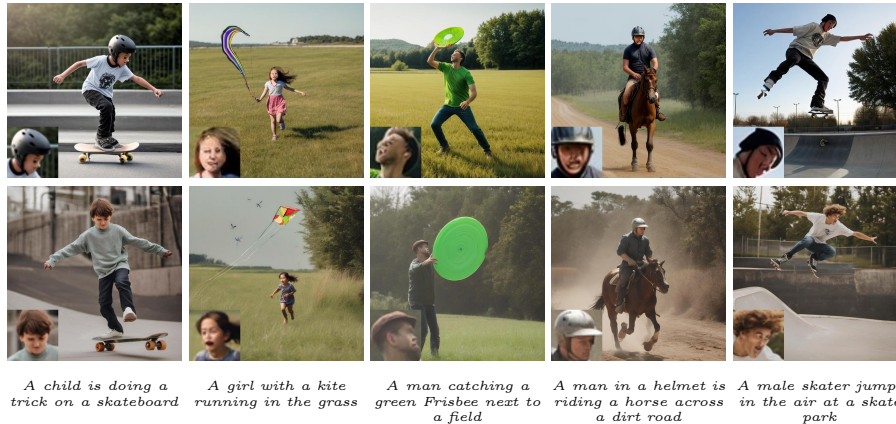


**Fig. 1:** Bad face cases generated by Realistic Vision V5.1 [40] (the first row) and SDXL [31] (the second row) with prompts below. Faces, especially small-scale faces, are highly likely to be vague and irrational. We enlarge the face region and place it in the bottom left corner of the image. Zoom in for more face details.

achieved unprecedented success due to their exceptional ability to generate content that surpasses human imagination.

Users may appreciate imaginative generations in creative scenarios, where factual inaccuracies can be tolerated. However, the expectation changes when it comes to capturing the realism of intricate details, where distorted generations are routinely unacceptable. In particular, the generated bad faces, especially the small-scale ones (see Fig. 1), are one of the most prominent issues for the people-oriented application of DMs. The possible causes of bad faces include that (1) faces encompass numerous complex details, while their proportion within an image is often too small for DMs to attend to; (2) the amount of images containing small-scale faces is usually limited for model training, and such images often pertain to chaotic and messy scenarios, which might cause aesthetic filters to exclude them.

To comprehensively investigate the bad face issue, we first empirically evaluate the face quality of generations from the prevalent Stable Diffusion V1.5 (SD1.5) [35], Realistic Vision V5.1 (RV5.1) [40], and SDXL [31]. We design a pipeline where human annotators rank the generated faces of the same prompt by different models and find that despite its smaller model size, RV5.1 achieves slightly superior results compared to SDXL. The evaluation results form a human preference dataset of face images, offering the possibility to quantify the alignment between human perception and existing popular metrics for synthetic images, including ImageReward (IR) [48], Human Preference Score (HPS) [47], Aesthetic Score Predictor (ASP) [8], and Face Quality Assessment (FQA) [27]. We observe that these metrics can be unsatisfactory in assessing the rationality

and aesthetic appeal of faces in synthetic images. That said, a new metric is urgently needed to bridge the gap.

The delivery of that metric entails access to a training dataset regarding face preference. To avoid the substantial cost and time required for human annotation, we innovatively devise an automatic pipeline for dataset construction based on the aid of the inpainting capacity of off-the-shelf pre-trained DMs—for a natural image containing faces, we detect, mask, and inpaint the face regions to gain an image with degraded faces and hence a (good, bad) face pair. With such pairs, we fine-tune the typical ImageReward to a novel *Face Score (FS)* metric. Extensive studies reveal that *FS* enjoys a superior alignment with humans over existing metrics, allowing for the automatic evaluation of the quality of future-generated faces without human intervention.

With *FS* as a target, we then advocate fine-tuning pre-trained DMs to enhance the face quality in text-to-image generation. We frame such a problem as a trajectory correction one, where the DM is tailored to be able to map points on the denoising trajectories of bad faces to trajectories of the corresponding good faces. We propose a guidance loss, applied to the constructed (good, bad) face pairs, to achieve this. Intuitively, our approach takes a low-quality image as input and teaches the DM how to escape from its original denoising trajectory. Comprehensive experiments verify the efficacy of our approach for improving face quality while preserving general capability.

In summary, our contributions can be listed as follows:

- We perform the first investigation of the bad face issue of DMs and systematically assess a range of image quality metrics for quantifying face quality.
- We propose *Face Score* to better quantify the quality of generated faces, which surpasses existing metrics with a decent margin.
- We propose a guidance loss to fine-tune DMs for generating higher-quality faces and verify its efficacy on both SD1.5 and RV5.1.

## 2 Related Works

**Text-to-image diffusion models.** Text-to-image (T2I) pre-trained diffusion models [28, 34, 35, 38] have undergone rapid developments and witnessed widespread applications. Given appropriate prompts as guidance, T2I DMs can generate visually appealing and semantically coherent images. While T2I DMs excel at capturing the overall essence and content of the given prompts, they often struggle to generate intricate details and fine-grained features.

**Diffusion model fine-tuning and evaluation.** Finetuning has empowered specific capabilities of DMs, such as extra image condition control [49], adaptability to personal styles or figures [18, 37], instruction following [5], alleviation on gender and race bias [41]. Aligning DMs with human preferences by fine-tuning is in emergence. DMs can learn what humans find appealing by utilizing publicly available text-image datasets with annotations, such as Pick-a-pic [19] and the Human Preference Dataset (HPD) [47]. Reward function gradients [9, 48] and reinforcement learning methods [3, 13] can also be applied. Paralleling the

alignment of large language models with human preference, direct preference optimization [33] is also adopted as a counterpart for diffusion models [46]. Still, they often fail to generate satisfactory small-scale faces.

Meantime, for evaluation, HPS [47] and IR [48] bridge the gap for human preference object metrics. They individually fine-tune CLIP [32] and BLIP [21] as the backbone models to score the images for the degree of human preference. However, these metrics focus on aesthetic appeal globally instead of local areas like faces, ignoring details generation. Furthermore, the lack of a comprehensive human preference dataset for faces also hampers the progress in improving face quality in synthetic images. In this work, we contribute a human preference dataset and an objective metric specifically for faces.

**Detail generation.** Previous studies have acknowledged the problem of detail generation like incorrect hands in DMs [31]. HandRefiner [24] leverages a lightweight post-processing solution and utilizes ControlNet [49] modules to re-inject correct hand information for inpainting. Likewise, ControlNet is incorporated to provide more guidance information to restore misshaped hands [50]. However, very few studies are on the topic of the bad face issue. To the best of our knowledge, we are the first to focus specifically on face generation.

### 3 Preliminary

Let  $x \in \mathcal{X}$  denote a natural image, i.e.,  $x \sim p_{data}$ . Diffusion models (DMs) gradually add Gaussian noise to  $x$  in the forward process and are trained to perform denoising to achieve image generation [16, 43]. Typically, the forward process takes the following transition kernel

$$q(x_t|x_{t-1}) = \mathcal{N}(x_t; \sqrt{\alpha_t}x_{t-1}, \beta_t I), t = 1, \dots, T, \quad (1)$$

where  $x_0 := x$  and  $\beta_t$  is the noise variance following a pre-defined schedule and  $\alpha_t = 1 - \beta_t$ . The forward process eventually renders  $x_T \sim \mathcal{N}(0, I)$ , i.e., the final state  $x_T$  amounts to a white noise. The generation process of DMs reverses the above procedure with a  $\theta$ -parameterized Gaussian kernel:

$$p_\theta(x_{t-1}|x_t) = \mathcal{N}(x_{t-1}; \mu_\theta(x_t, t), \beta_t I), t = T, \dots, 1, \quad (2)$$

where the Gaussian variance is set to  $\beta_t I$  for simplicity following [16]. It can be learned as well. The mean prediction model  $\mu_\theta(x_t, t)$  can be parameterized as a noise prediction one  $\epsilon_\theta(x_t, t)$  [16], which is usually implemented as a U-Net [36].

After training, we can first draw a random sample  $x_T \sim \mathcal{N}(0, I)$  and iterate over the above transition kernel to obtain an image sample. Such a sampling process can be viewed as a discretization of a reverse-time stochastic differential equation (SDE), and there is a corresponding probability flow ordinary differential equation (PF-ODE) sharing the same marginal probability densities [44]. The DDIM sampler [42] is a typical ODE-based one in the following form:

$$x_{t-1} = \sqrt{\bar{\alpha}_{t-1}}\bar{x}_0 + \sqrt{1 - \bar{\alpha}_{t-1}}\epsilon_\theta(x_t, t), t = T, \dots, 1, \quad (3)$$

where  $\bar{\alpha}_k = \prod_{i=1}^k \alpha_i$  and  $\bar{x}_0$  is the predicted  $x_0$  by one-step denoising:

$$\bar{x}_0 = \frac{x_t - \sqrt{1 - \bar{\alpha}_t} \epsilon_\theta(x_t, t)}{\sqrt{\bar{\alpha}_t}}. \quad (4)$$

For efficient training and sampling, DMs can be shifted in the latent space [35] with the help of an auto-encoder [12]. Specifically, the image  $x$  is first projected by the encoder to a low-dimensional latent representation  $z = \mathcal{E}(x)$ , and  $z$  can be projected back to the image space by a decoder.

## 4 Human Preference on Generated Face Images

In this section, we first expose the bad face issue of existing DMs and test how good existing image-wise metrics are for quantifying the face quality of synthetic images. We then develop *Face Score (FS)* as a more qualified metric to assess the rationality and aesthetic appeal of generated face images.

### 4.1 The Bad Face Issue

The difficulties of DMs for generating intricate details, especially realistic human faces and hands, are no longer novel [31]. As shown in Fig. 1, images generated by RV5.1 [40] and SDXL [31] usually contain distorted faces. As previously mentioned, the issue may originate from the scarcity of face data in model training or the fact that the face regions are relatively small compared to the whole image but need to contain intricate details. In general, to generate images with human faces, it is a common practice to introduce negative prompts based on the classifier-free guidance (CFG) technique [17] of DMs to increase the chances of generating high-quality faces. Fig. 2 displays results regarding this, where we see negative prompts indeed contribute to enhancing the face quality but the generated faces are still unsatisfactory. Practitioners may perform DM-based inpainting [1, 35] to specifically re-generate the face regions, but the faces can still be low-quality due to the fundamental issue of the poor face generation capability of existing DMs.

### 4.2 Evaluation of Existing DMs

Next, we conduct a detailed manual evaluation of the face generation quality across three popular DMs: SD1.5 [35], RV5.1, and SDXL. Specifically, we leverage the following pipeline for evaluation:

1. select 1k prompts related to human subjects in the MS-COCO 2017 5K validation dataset [22], which includes descriptions of human-centric in&outdoor scenes and ,single&multi-person scenarios;
2. for each prompt, generate a triplet of images (see Fig. 3 for an example) with the three DMs (the triplet is discarded if there are no valid faces in any image);



**Fig. 2:** Comparison between generations sampled without (left) and with (right) negative prompts from Realistic Vision V5.1 [40]. Experiments are under the same conditions except for negative prompts, set as “bad face, deformed, poorly drawn face, mutated, ugly, bad anatomy”. Enhancement can be observed in the face region with negative prompts. However, the generation still suffers from low quality. Zoom in for more face details.

**Table 1:** Face quality comparisons between SD1.5, RV5.1, and SDXL. We present the proportion of each kind of score as well as the average score of each model.

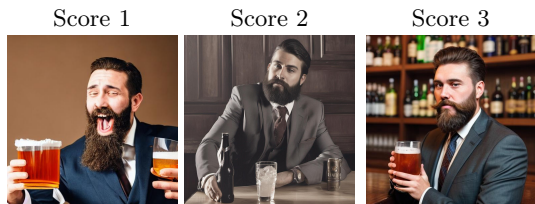
Models	Score 1 (%)	Score 2 (%)	Score 3 (%)	Average score
SD1.5	76.20	18.65	5.15	1.2895
RV5.1	12.22	37.20	50.58	<b>2.3836</b>
SDXL	11.58	44.16	44.26	2.3268

- introduce five human annotators to individually rank the triplet of each prompt based on face quality; the best image in the triplet receives a score of 3 and the worst receives a score of 1;
- integrate the annotation results based on majority voting.

To determine the preference alignment of the five annotators and make the annotation more convincing, we compute the frequency of more than three annotators among the five as signing the same label to the image to quantify the annotators’ agreement and obtain 93.3%. The integration further helps to mitigate the impact of individual biases and achieve alignment with population preferences. Fig. 3 presents an example of the annotated triplet and Tab. 1 displays the statistics of human preference over the three DMs. As shown, although the face quality of RV5.1 is not good enough (see Fig. 2), it still slightly surpasses the larger SDXL, which strengthens the concerns about the bad face issue of existing DMs. On the other hand, SD1.5 falls significantly behind the other two DMs.

### 4.3 Evaluation of Existing Metrics

A good metric can enable the automatic, scalable evaluation of the face quality of the generations, avoiding expensive and time-consuming labeling processes by humans and paving the way for the development of new models. We then



*Bearded man in a suit about to enjoy an adult beverage*

**Fig. 3:** An example of the human-annotated triplet. The image with higher face quality is assigned a higher score. In each triplet, there are 3 binary comparisons.



*A man in a suit and tie standing up*

**Fig. 4:** An example of a face pair. We leverage the inpainting pipeline for a degraded version, thereby forming a (good, bad) face pair.

investigate this—evaluating how well existing image-wise metrics are aligned with human preference on generated faces, based on the above annotated triplets.

Concretely, we concern ImageReward (IR) [48], Human Preference Score (HPS) [47], Aesthetic Score Predictor (ASP) [8], and Face Quality Assessment (FQA) [27], which are prevalent for evaluating human preference or aesthetic quality in text-to-image generation. Intuitively, HPS and IR concentrate on the global image instead of the local area, so they are not suitable for evaluating the quality of generated faces. Thereby, we also develop variants of them, i.e., LocalHPS and LocalIR, where we detect the local face regions with a detector [10] and send them into the original scoring pipeline with a default prompt “A face” for specific face evaluation.

We are majorly interested in the relative relationships of the metric evaluations on various images instead of the absolute numerical values. Consequently, we build a small dataset containing roughly 3k annotated triplets, where each triplet forms two pairwise comparisons. For metric evaluation, we calculate the accuracy of the binary ranking based on the metric compared with the human ranking for the data pairs. We list the results in Tab. 2. We can observe that the performance of IR and ASP is unsatisfactory, perhaps due to their more attention on global image features, and LocalIR performs slightly better. FQA is poor as well because it is applied to evaluate the suitability of the face images for recognition and hence can be biased for the assessment of human preference on generated faces. HPS and LocalHPS are the best among the metrics. Nonetheless, the up to 75.31% accuracy still leaves considerable room for further improvement.

#### 4.4 Face Score: a New Metric for Synthetic Face Images

Given the above findings, we aim to develop a new metric to quantify the quality/human preference of synthetic face images. We dub such a metric as *Face Score (FS)* and expect it to correlate with both the rationality and aesthetic appeal of face generations. To achieve this, we construct a preference dataset on

**Table 2:** Ranking alignment of existing popular metrics with human preference on generated face images. We also include the proposed *Face Score (FS)* into comparison.

Methods	Backbone	Prompt input	Acc.(%)
Random guess	–	✗	50.00
IR [48]	BLIP	✓	60.87
ASP [8]	CLIP	✗	68.81
FQA [27]	–	✗	70.22
LocalIR [48]	BLIP	✓	71.27
HPS [47]	CLIP	✓	74.70
LocalHPS [47]	CLIP	✓	75.31
<i>FS</i> (ours)	BLIP	✓	<b>80.31</b>

face images in an automatic and scalable way, based on which we perform model fine-tuning to obtain *FS*.

**Dataset construction.** Though open-source human preference datasets can be applied to training the evaluation models involved in the metric, they are not specifically for faces. On the other hand, our collected human annotations are limited in amount because the labeling process is both costly and time-consuming, so the resultant data can be primarily used for evaluation instead of model training. To address such issues, we propose a new collection pipeline for face preference data, based on the inpainting capacity of off-the-shelf pre-trained DMs. Specifically, we

1. for natural images containing human faces in the LAION dataset [39], detect the face regions using detectors [10], obtaining face masks  $M$ ;
2. mask out and inpaint the face regions with an inpainting pipeline [11, 35].

We plot the procedure in the middle column of Fig. 6. The underlying hypothesis behind this method is that the face quality of an inpainted image  $x^b$  is worse than that of the original one  $x^g$ . This can be easily fulfilled by controlling the noise factors involved in the inpainting pipeline, and we have empirically verified this (see Fig. 4). The above pipeline eventually produces a dataset  $\mathcal{D}$  of 375k  $(x^g, x^b)$  pairs based on 197k natural images.

**Ranking loss.** We then would like to learn a scorer  $s_\phi : \mathcal{X} \rightarrow \mathbb{R}$  to fit the preference dataset  $\mathcal{D}$ . Drawn inspiration from the modeling of human preference over the aesthetic appeal of generated images [48], we utilize a naive ranking loss to tune  $s_\phi$ . Specifically, given a random mini-batch  $\mathcal{B}$  from  $\mathcal{D}$ , we minimize the following loss:

$$L_{rank}(\phi) = -\frac{1}{|\mathcal{B}|} \sum_{(x^g, x^b) \in \mathcal{B}} [\log(\sigma(s_\phi(x^g) - s_\phi(x^b)))], \quad (5)$$

---

We can also input the text prompt corresponding to the image  $x$  to the scorer, but omit it here for simplicity.





**Fig. 5:** Some randomly selected face images and the corresponding  $FS$ . We see a positive correlation between the score and the rationality and aesthetic appeal of faces.

where  $\sigma(\cdot)$  denotes the sigmoid function. Other possible learning principles are left as future work.

**Fine-tuning IR.** Considering the prevalence of IR and the improved capacity of BLIP architecture [21] over conventional CLIP [32] for modeling human preference [48], we adopt IR to initialize our scorer  $s_\phi$  and then perform fine-tuning to avoid the cold start problem. Noting that we only care about the quality of faces rather than the properties of the whole image, we detect faces in the image, as done in LocalIR, and tune the model on only the face regions. The prompt is set to “A face” by default. We freeze the first 70% layers of the transformer [45] backbone and train with a learning rate of 1e-5 and a batch size of 64 on a single 80G A800 GPU.

**Quantitative comparisons.** We first report the accuracy of  $FS$  to rank human-annotated images in Tab. 2. We see  $FS$  gets the best accuracy compared to existing metrics, so it can serve as a better metric for evaluating faces in synthetic images. In Fig. 5, we illustrate some randomly selected face images and the corresponding  $FS$ s, which implies that rationality and aesthetic appeal of faces are positively correlated with  $FS$ . To show the generalization of evaluating face quality, we also report  $FS$  in Tab. 3 for different open-source and close-source text-to-image diffusion models, which generate images in the same manner as the test set. We observe PGV2.5 gets the best  $FS$ . It makes sense since its authors claim that the image quality is better than MJ’s. We also conclude that the face generation quality and the overall generation quality of the models are positively correlated.

**Table 3:**  $FS$  statistic on more text-to-image diffusion models. SC is for Stable Cascade, PGV2.5 for Playground V2.5, MJ for Midjourney, Real for real faces from COCO.

Model	Dalle3	MJ	Real	PixArt- $\alpha$	SC	PGV2.5
$FS$	3.45	3.51	3.54	3.94	3.98	4.40

We also calculate the detailed statistics of  $FS$  in BLIP architecture, compared with LocalHPS in CLIP architecture, and FQA, for the images in the human-annotated dataset. We normalize the output scores to  $[0, 1]$  for each metric and

**Table 4:** Statistical alignment with human preference. We report pearson correlation(PC) between the human ranking and the metrics. We also report the median instead of the mean of the scores for images generated by each DM following [48]. We can observe that PC between FS and human ranking is the highest compared to other metrics. Besides, *FS* aligns perfectly with human ranking and exhibits higher variance than HPS, which reflects its better human alignment and higher distinguishability.

Model	PC	Statistics	SD1.5 [35]	RV5.1 [40]	SDXL [31]
FQA [27]	0.4626	Median	0.1600	0.2980	0.3723
		Std	0.2173	0.2864	0.3206
<i>LocalHPS</i>	0.5715	Median	0.4206	0.4591	0.3877
		Std	0.1441	0.1625	0.1448
<i>FS</i>	0.6759	Median	0.5673	0.7993	0.7775
		Std	0.2575	0.2557	0.1994

report the statistics corresponding to images from various DMs individually in Tab. 4. As shown, the median of FQA fails to accurately represent the quality of faces. Conversely, the median of *FS* can better align with the average score given by humans. Moreover, it can showcase the subtle differences between RV5.1 and SDXL, and indicate the much weaker performance of SD1.5. Besides, compared with LocalHPS, *FS* exhibits a larger variance, implying its stronger ability to differentiate the quality of face images.

## 5 Improving Face Quality by Fine-tuning DMs

In this section, we elaborate on the proposed guidance loss to fine-tune DMs as well as some critical optimization strategies.

In DMs, the sampling process of an image naturally produces a trajectory, particularly a deterministic ODE trajectory when adopting efficient ODE-based samplers such as DDIM [42]. Intuitively, the DDIM trajectories of two images, which hold striking similarities but contain good and bad faces respectively, can be close. That said, we can try to guide the trajectory of the bad image to that of the good one at a minimal cost to prevent distorted generations. Luckily, the numerous  $(x^g, x^b)$  pairs constructed before open the opportunities for realizing this objective. As a result, we implement a guidance loss to correct pre-trained DMs for generating better faces.

Specifically, let  $\epsilon_{\theta^*}(z_t, t)$  and  $\epsilon_{\theta}(z_t, t)$  denote the original DM and the DM for fine-tuning respectively. For a pair of images  $(x^g, x^b)$ , we first transform them into latent codes  $z_0^g = \mathcal{E}(x^g)$  and  $z_0^b = \mathcal{E}(x^b)$  and properly downsample the face mask  $M$  to  $m$  in the processing of latent diffusion models. We then add Gaussian noise to the latent codes to obtain  $z_t^g = \sqrt{\alpha_t}z_0^g + \sqrt{1 - \alpha_t}\epsilon$  and  $z_t^b = \sqrt{\alpha_t}z_0^b + \sqrt{1 - \alpha_t}\epsilon$ , with  $\epsilon \sim \mathcal{N}(0, I)$ . Note that the same noise is applied to both images to guarantee that the resulting hidden states lie close to each other, and hence belong to adjacent DDIM trajectories. Based on the iteration rule of

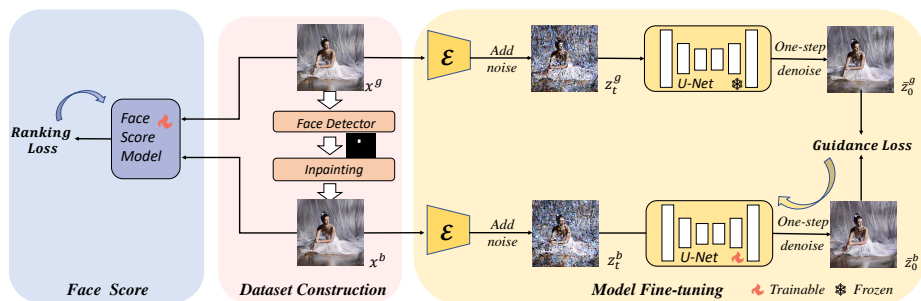


**Fig. 6:** Method overview. The middle box refers to the construction of a large-scale preference dataset for face images. A natural image containing faces undergoes face detection and inpainting processes to obtain a (good, bad) face pair. The left box shows that the face pairs are utilized to fine-tune a scorer using a ranking loss for face quality evaluation. The right box illustrates the pipeline where we introduce guidance loss to correct the DDIM sampling trajectory that leads to a bad face. Note that though we use the notation  $z$ , some shown images are decoded back to image space for visualization.

DDIM detailed in Eqs. (3) and (4), we decide to push the one-step denoising outcome of  $z_t^b$  to that of  $z_t^g$ . In particular, the former should be constructed with  $\epsilon_\theta(z_t, t)$  for model fine-tuning; we produce the latter with the original DM  $\epsilon_{\theta^*}(z_t, t)$  to establish a constant target. Namely,

$$\bar{z}_0^b = \frac{z_t^b - \sqrt{1 - \bar{\alpha}_t} \epsilon_\theta(z_t^b, t)}{\sqrt{\bar{\alpha}_t}}, \quad \bar{z}_0^g = \frac{z_t^g - \sqrt{1 - \bar{\alpha}_t} \epsilon_{\theta^*}(z_t^g, t)}{\sqrt{\bar{\alpha}_t}}. \quad (6)$$

We then minimize the following guidance loss

$$L_{guidance}(\theta) = d(m \circ \bar{z}_0^g, m \circ \bar{z}_0^b), \quad (7)$$

where the face mask  $m$  is applied in an element-wise manner to ensure the focus on faces and  $d(\cdot, \cdot)$  denotes a distance measure. One of the common choices for  $d$  is the  $\ell_2$  distance. Except for that, we can decode the latent codes  $\bar{z}_0^g$  and  $\bar{z}_0^b$  back to the image space and then extract the semantics with a pre-trained feature extractor such as DINO [6] to measure the semantical disparities between them.

In addition to the guidance loss, we also provide insights on two crucial factors for model optimization below.

- **Timesteps.** We visualize the evolvement of face images in the sampling process in Fig. 7, and notice that in the early stage of sampling, the layout and colors are rendered while the details have not yet emerged. As the sampling process progresses, the details gradually recover and elaborate. This enlightens us to keep the forward timestep  $t$  relatively small to avoid wasting optimization efforts on too noisy states. From Fig. 7, we can observe that the emergence of finer details occurs approximately midway through the inference process, so empirically we take  $t \sim U[1, 0.5T]$  for fine-tuning DMs, where  $U[a, b]$  is the uniform distribution over the interval  $[a, b]$ .



**Fig. 7:** Denoised images at different timesteps. The prompt is “A kid and a girl are next to each other” and the total number of sampling steps is set to 50. The number of sampling steps increases from left to right, with an interval of 10. We observe that the recovery of layout information is more prominent at the early stage of sampling while details (including those in human faces) are generated at the later stages.

- **Self-attention layers.** Intuitively, the cross-attention layers in DMs capture the correlation between images and texts, while the self-attention ones cope with the interdependencies within the image itself. With these, we particularly optimize the parameters of the self-attention layers in the U-Net of DMs for face quality enhancement.

## 6 Experiments

### 6.1 Experiment Settings

**Training setting.** We conduct experiments on SD1.5 and RV5.1 and only leverage the guidance loss. Since RV5.1 is a fine-tuned version of SD1.5 and generates better images especially faces than SD1.5, we set the learning rate  $1e-5$  for SD1.5 and  $1e-6$  for RV5.1. The models are fine-tuned on 4 80GB NVIDIA A800 GPUs, with batch size of 2 and gradient accumulation of 8. During training, we set 20% dropping of the text-conditioning. We leverage two distance metric measures, one of which is  $\ell_2$  distance, and the other one is DINO [6] feature distance.

**Evaluation Settings.** For the evaluation of general capability, we leverage MJHQ-30K dataset [30] and sample 5k prompts from each category equally and report CLIP-Score, IR and HPS for comparisons. Since there are no fine-tuning methods specifically for faces, we only take the base model and DPO [46] as baselines. To evaluate face quality, we sample images given prompts from the evaluation dataset and report the mean of  $FS$  for each DM. We use PNDM [23] noise scheduler and default CFG scale of 7.5 and steps of 50 for inference.

### 6.2 Results and Analysis

We present the quantitative comparisons in Tab. 5. As demonstrated, for SD1.5, both ours- $\ell_2$  and ours-DINO outperform the base model [35] concerning all of the four metrics by a large margin, indicating that the proposed guidance loss is capable of enhancing not only overall image quality but also generated face quality. Compared with DPO methods, we observe slightly lower CLIP-Score and HPS in (ours- $\ell_2$ ), potentially due to the utilization of global optimization loss in DPO. However, in terms of face quality, our methods achieve the higher *Face Score*, which showcases the better generation ability of faces. We emphasize

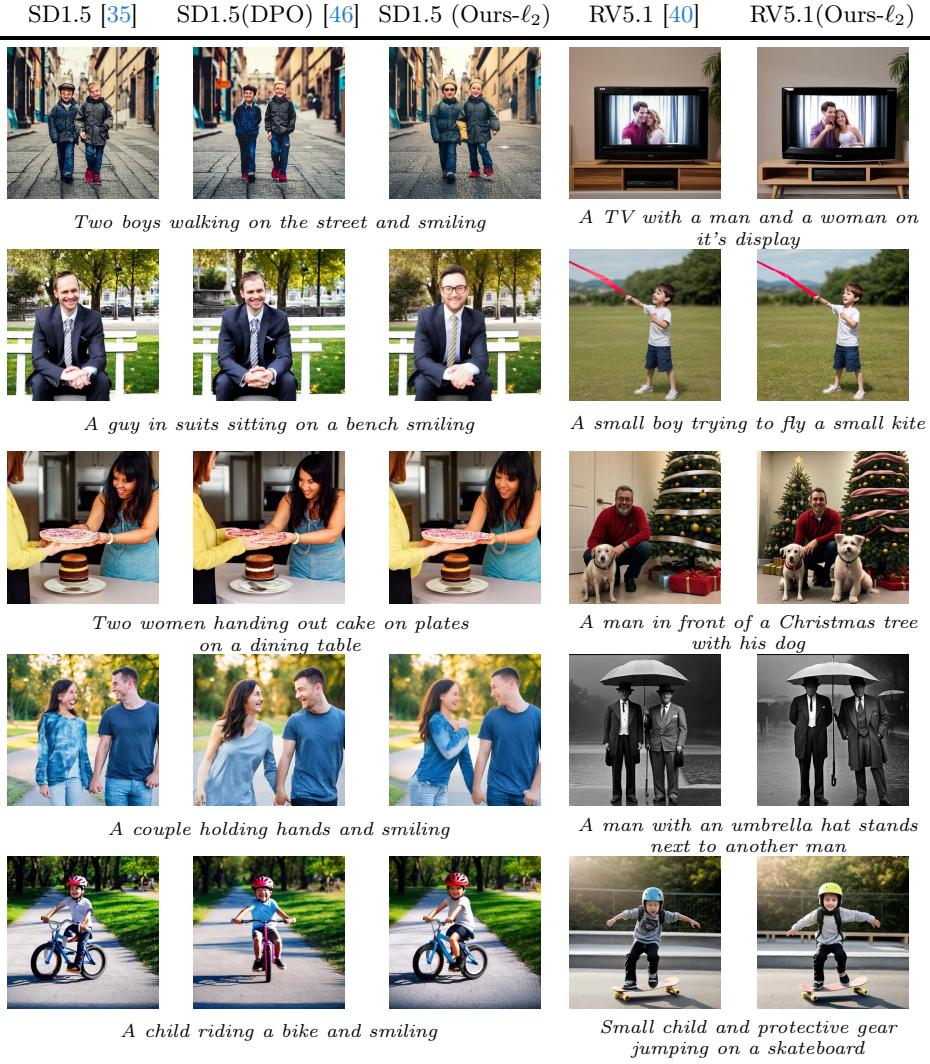


**Fig. 8:** Qualitative comparisons between our methods and baselines with base models SD1.5 and RV5.1. The sampling is under the same settings as the prompts below. We observe a significant improvement in face quality through our method compared with the baselines while preserving the semantic information.

**Table 5:** Generation performance comparisons between our method and competing baselines. CLIP-Score measures the alignment between prompts and images. IR and HPS assess the aesthetic quality and the degree of human preference, and our *FS* evaluates the face quality. For SD1.5, we improve the overall image quality compared with the baselines and significantly enhance face quality. For RV5.1, our method can refine faces while keeping the general capability.

Base model	Method	CLIP-Score $\uparrow$	IR $\uparrow$	HPS $\uparrow$	FS $\uparrow$
SD1.5 [35]	Base [35]	0.3098	-2.22	0.2030	0.3111
	DPO [46]	<b>0.3189</b>	1.53	<b>0.2942</b>	0.7720
	Ours- $\ell_2$	0.3148	<b>1.56</b>	0.2860	<b>1.4683</b>
	Ours-DINO	0.3153	1.15	0.2825	1.1431
RV5.1 [40]	Base [40]	0.3252	1.76	0.3342	2.7349
	Ours- $\ell_2$	0.3247	1.76	<b>0.3425</b>	<b>2.9941</b>
	Ours-DINO	<b>0.3253</b>	<b>1.77</b>	0.3350	2.8653

that our work focuses on enhancing the quality of face generation rather than improving the overall quality of the images. For RV5.1, compared to the base model, our methods obtain better IR and HPS and comparable CLIP scores, significantly upgrading *FS*. This result again demonstrates our methods can simultaneously improve general generative capability and synthetic face quality. We also visualize some qualitative results to show the superiority of our methods in the improvement of face quality in Fig. 8. We can observe that compared with baselines, the improvement in face quality is remarkable, in terms of rationality, clearness, and aesthetic appeal.

### 6.3 Ablation

We discussed before that timesteps and self-attention layers are crucial for detail generation as well as face generation. We conduct the following ablation study with RV5.1 and DINO feature distance metric measure.

**Timesteps.** To demonstrate the effectiveness of selectively choosing from relatively small timesteps for fine-tuning, we additionally fine-tune DMs under the condition of randomly selecting from all the timesteps while keeping others the same. From Tab. 6, we can see that in face quality comparison, considering only the relatively small timesteps is more effective. The reason is that as the timestep decreases and approaches zero, the generation process of finer details begins, and focusing on them helps better detail generation as well as face generation. More ablation studies about timesteps will be included in the supplementary materials.

**Self-attention layers.** Theoretically, self-attention layers have a greater impact on face generation. To prove it experimentally, we compare Ours-DINO with full fine-tuning. From Tab. 6, we can see that Ours-DINO with self-attention fine-tuning outperforms full fine-tuning, proving that self-attention takes a significant

**Table 6:** Ablation study. We observe that only optimizing relatively small timesteps and self-attention layers achieve better face quality while optimizing all timesteps or performing full fine-tuning results in a slight decline in performance.

Method	CLIP-Score $\uparrow$	IR $\uparrow$	HPS $\uparrow$	<i>FS</i> $\uparrow$
Ours-DINO	0.3253	1.77	0.3350	<b>2.8653</b>
All timesteps	0.3251	1.62	0.3376	2.6980
Full fine-tuning	0.3253	1.70	0.3325	2.7816

role in generating details. We believe that self-attention not only enhances image quality but also facilitates the generation of finer details.

## 7 Conclusion

In this work, we focus on the bad face issue raised by diffusion models and discuss the possible reasons and common ways to alleviate it. We evaluate face generation quality across popular diffusion models. We also assess the effectiveness of existing image-based metrics in quantifying the quality of synthetic images but encounter unsatisfactory results in face evaluation. To fill up the vacancy in this field, we propose a ranking dataset annotated by human evaluation and a large-scale dataset of (good, bad) face pairs constructed implicitly without annotations. Except for datasets, we develop a new metric named *Face Score* specifically for the evaluation of rationality and aesthetic appeal of faces in the synthetic images trained on the face pair dataset. With such a metric, a fine-tuning method for better face generation by correcting the trajectory is also proposed. Through our complete workflow, we help to better align text-to-image generation with human preference for face generation.

Though the methodology can be generalized to detail generation, we only focus on face generation quality in this work. Further research is required to address other detailed generation issues, such as problems related to hand quality. Additionally, we can explore more choices of distance metrics and the form of the guidance loss. They are left as future works.

## 8 Appendix

### 8.1 Algorithm

We leverage the face pairs for fine-tuning DMs. A corresponding mask  $m$  indicates the location of the face in the image while the prompt  $p$  provides a description of the content of the image. The fine-tuning algorithm is presented in the Algorithm 1. We provide more results in Fig. 9.

---

**Algorithm 1:** Fine-tune DMs by Face Pairs
 

---

```

1: Input: Dataset  $D = \{(z^g, z^b, m, p), \dots\}$ , the original DM  $\epsilon_{\theta^*}(z_t, t)$ ,
   the target DM  $\epsilon_{\theta}(z_t, t)$ , the distance measure function  $d$ 
2: Initialization: The noise scheduler, the number of noise scheduler timestep  $T$ 
3: for each  $(z^g, z^b, m, p)$  in  $D$  do
4:    $t \leftarrow \text{rand}(0, 0.5T)$ ,  $\epsilon \sim \mathcal{N}(0, I)$ 
5:    $z_t^g, z_t^b \leftarrow \text{Forward}(z^g, t, \epsilon), \text{Forward}(z^b, t, \epsilon)$  // Add noise to images
6:   no grad:  $\bar{z}_0^g \leftarrow \text{OneStepDenoise}(z_t^g, \epsilon_{\theta^*}(z_t^g, t))$  // Predict  $\bar{z}_0^g$ 
7:   with grad:  $\bar{z}_0^b \leftarrow \text{OneStepDenoise}(z_t^b, \epsilon_{\theta}(z_t^b, t))$  // Predict  $\bar{z}_0^b$ 
8:    $L_{\text{guidance}} \leftarrow d(m \circ \bar{z}_0^g, m \circ \bar{z}_0^b)$ 
9:   Update  $\epsilon_{\theta}$  based on  $L_{\text{guidance}}$ 
10: end for
11: return The fine-tuned DM  $\epsilon_{\theta}$ 

```

---

### 8.2 More Ablation Studies on Timesteps

In the paper, we conduct ablation studies on timesteps. Here we provide more detailed ablation studies on them. To explore the optimal strategy for achieving better face generation or detail generation, we consider different timestep splitting points  $T_{\text{end}}$  and take 250 as a unit. Specifically, we choose from timestep 0 to  $T_{\text{end}}$ , i.e., taking values from 250, 500, 750, and 1000. The experiments take RV5.1 as the base model and DINO feature distance as the measure. Except for the  $T_{\text{end}}$ , we keep other settings unchanged and take the same comparison settings.

As shown in Tab. 7, as  $T_{\text{end}}$  increases, the detail generation performance, which we focus on and is indicated by *Face Score*, exhibits an initial increase followed by a continuous decrease, and  $T_{\text{end}} = 500$  is optimal, so we adopt it as the default setting in other experiments. The reason why the detail generation is better when  $T_{\text{end}} = 750$  compared to when  $T_{\text{end}} = 250$  may be attributed to the fact that  $T_{\text{end}} = 750$  includes the interval of  $T_{\text{end}} = 500$ . As for the other metrics, their focus is primarily on the overall aesthetic quality, which is not within our scope of concern, rather than the specific face details.



**Table 7:** A more detailed ablation study on timesteps.

$T_{end}$	CLIP-Score $\uparrow$	IR $\uparrow$	HPS $\uparrow$	$FS$ $\uparrow$
250	0.3251	1.80	0.3403	2.8309
500	0.3253	1.77	0.3350	<b>2.8653</b>
750	0.3249	1.78	0.3306	2.8395
1000	0.3251	1.62	0.3376	2.6980

### 8.3 Datasets

To provide a more intuitive understanding of the dataset, we present some details about the process of dataset formation and extract a subset of samples to help readers gain a preliminary understanding of the format and quality of the dataset, and better comprehend the methods and results presented in our paper.

### 8.4 Ranking Criteria for Evaluation

We establish the following annotation rules for human annotators:

- Discard those triplets if there are no valid faces in any image;
- Focus solely on the faces and do not need to consider the alignment between the prompt and the image, the aesthetic aspect of the image itself, or any other irrelevant factors;
- Prioritize the rationality of the face before considering its aesthetic aspect.
- Select the most frontal and representative face for comparison purposes in multi-person scenes.

We also provide more image triplets in Fig. 11 to see the correlation between face quality and human preference.

**Face Pairs Construction** In the inpainting pipeline of DMs, the noise factor is a hyper-parameter, which should be chosen carefully. We intend to degrade the face to resemble the quality of a bad face generated by DMs. Experimentally, we find that an increased noise factor leads to more pronounced degradation, and different sizes of faces exhibit varying levels of resistance to the degradation effects. To this end, we choose various noise factors based on the proportion of the face in the image as shown in Tab. 8. We go through multiple rounds of data filtering, including the removal of faces that are too small and blurry, as well as other invalid faces. We present more examples in the implicit human preference dataset of faces in Fig. 12.

### 8.5 Face Generation Quality

**Evaluation Discussion** We observe a positive correlation between the quality of generated faces and the aesthetic quality of their corresponding images, which

**Table 8:** Different face area ratios correspond to various noise factors.

Face area ratio	(0, 0.5%]	(0.5%, 1%]	(1%, 10%]	(10%, 100%]
Noise factor	0.06	0.1	0.2	0.4

is influenced by the model’s capabilities. This correlation can be explained by the fact that stronger models exhibit a higher capacity for generating finer details and explains why IR and HPS can perform better than random guesses on predicting human preference on faces, though they are designed and trained on the whole image and focus on the global features.

**Face Score Discussion** We provide additional examples in Fig. 10. It can be seen that when *Face Score* is higher than about 4, the generated faces are generally plausible. Moreover, the higher the score, the more attractive the faces tend to be, albeit in different ways. Conversely, when the score falls below 4 and continues to decline, the faces are no longer satisfactory or realistic. At first, the faces may appear slightly blurry and exhibit some distortion in certain details. Eventually, significant blurriness causes the faces to become unrecognizable. Based on the relationship between the *Face Score* and the quality of face generation, we can take it as a reliable automated evaluation metric for assessing the quality of face generation.

## References

1. Avrahami, O., Fried, O., Lischinski, D.: Blended latent diffusion. *ACM Transactions on Graphics (TOG)* **42**(4), 1–11 (2023) **1, 5**
2. Avrahami, O., Lischinski, D., Fried, O.: Blended diffusion for text-driven editing of natural images. In: *Proceedings of the IEEE/CVF Conference on Computer Vision and Pattern Recognition*. pp. 18208–18218 (2022) **1**
3. Black, K., Janner, M., Du, Y., Kostrikov, I., Levine, S.: Training diffusion models with reinforcement learning. *arXiv preprint arXiv:2305.13301* (2023) **3**
4. Blattmann, A., Dockhorn, T., Kulal, S., Mendeleevitch, D., Kilian, M., Lorenz, D., Levi, Y., English, Z., Voleti, V., Letts, A., et al.: Stable video diffusion: Scaling latent video diffusion models to large datasets. *arXiv preprint arXiv:2311.15127* (2023) **1**
5. Brooks, T., Holynski, A., Efros, A.A.: Instructpix2pix: Learning to follow image editing instructions. In: *Proceedings of the IEEE/CVF Conference on Computer Vision and Pattern Recognition*. pp. 18392–18402 (2023) **3**
6. Caron, M., Touvron, H., Misra, I., Jégou, H., Mairal, J., Bojanowski, P., Joulin, A.: Emerging properties in self-supervised vision transformers. In: *Proceedings of the International Conference on Computer Vision (ICCV)* (2021) **11, 12**
7. Chen, N., Zhang, Y., Zen, H., Weiss, R.J., Norouzi, M., Chan, W.: Wavegrad: Estimating gradients for waveform generation. In: *International Conference on Learning Representations* (2020) **1**
8. christophschuhmann: Aesthetic score predictor, <https://github.com/christophschuhmann/improved-aesthetic-predictor>, Last accessed on 2024-02-28 **1, 2, 7, 8**
9. Clark, K., Vicol, P., Swersky, K., Fleet, D.J.: Directly fine-tuning diffusion models on differentiable rewards. *arXiv preprint arXiv:2309.17400* (2023) **3**
10. Deng, J., Guo, J., Ververas, E., Kotsia, I., Zafeiriou, S.: Retinaface: Single-shot multi-level face localisation in the wild. In: *Proceedings of the IEEE/CVF conference on computer vision and pattern recognition*. pp. 5203–5212 (2020) **7, 8**
11. diffusers: Inpaint, <https://huggingface.co/docs/diffusers/using-diffusers/inpaint>, Last accessed on 2024-02-28 **8**
12. Esser, P., Rombach, R., Ommer, B.: Taming transformers for high-resolution image synthesis. In: *Proceedings of the IEEE/CVF conference on computer vision and pattern recognition*. pp. 12873–12883 (2021) **5**
13. Fan, Y., Watkins, O., Du, Y., Liu, H., Ryu, M., Boutilier, C., Abbeel, P., Ghavamzadeh, M., Lee, K., Lee, K.: Dpok: Reinforcement learning for fine-tuning text-to-image diffusion models. *arXiv preprint arXiv:2305.16381* (2023) **3**
14. Gupta, A., Yu, L., Sohn, K., Gu, X., Hahn, M., Fei-Fei, L., Essa, I., Jiang, L., Lezama, J.: Photorealistic video generation with diffusion models. *arXiv preprint arXiv:2312.06662* (2023) **1**
15. Ho, J., Chan, W., Saharia, C., Whang, J., Gao, R., Gritsenko, A., Kingma, D.P., Poole, B., Norouzi, M., Fleet, D.J., et al.: Imagen video: High definition video generation with diffusion models. *arXiv preprint arXiv:2210.02303* (2022) **1**
16. Ho, J., Jain, A., Abbeel, P.: Denoising diffusion probabilistic models. *Advances in neural information processing systems* **33**, 6840–6851 (2020) **1, 4**
17. Ho, J., Salimans, T.: Classifier-free diffusion guidance. *arXiv preprint arXiv:2207.12598* (2022) **5**
18. Hu, E.J., Shen, Y., Wallis, P., Allen-Zhu, Z., Li, Y., Wang, S., Wang, L., Chen, W.: Lora: Low-rank adaptation of large language models. *arXiv preprint arXiv:2106.09685* (2021) **3**

19. Kirstain, Y., Polyak, A., Singer, U., Matiana, S., Penna, J., Levy, O.: Pick-a-pic: An open dataset of user preferences for text-to-image generation. arXiv preprint arXiv:2305.01569 (2023) [3](#)
20. Kong, Z., Ping, W., Huang, J., Zhao, K., Catanzaro, B.: Diffwave: A versatile diffusion model for audio synthesis. arXiv preprint arXiv:2009.09761 (2020) [1](#)
21. Li, J., Li, D., Xiong, C., Hoi, S.: Blip: Bootstrapping language-image pre-training for unified vision-language understanding and generation. In: International Conference on Machine Learning. pp. 12888–12900. PMLR (2022) [4](#), [9](#)
22. Lin, T.Y., Maire, M., Belongie, S., Hays, J., Perona, P., Ramanan, D., Dollár, P., Zitnick, C.L.: Microsoft coco: Common objects in context. In: Computer Vision–ECCV 2014: 13th European Conference, Zurich, Switzerland, September 6–12, 2014, Proceedings, Part V 13. pp. 740–755. Springer (2014) [5](#)
23. Liu, L., Ren, Y., Lin, Z., Zhao, Z.: Pseudo numerical methods for diffusion models on manifolds. In: International Conference on Learning Representations (2021) [12](#)
24. Lu, W., Xu, Y., Zhang, J., Wang, C., Tao, D.: Handrefiner: Refining malformed hands in generated images by diffusion-based conditional inpainting. arXiv preprint arXiv:2311.17957 (2023) [4](#)
25. Lugmayr, A., Danelljan, M., Romero, A., Yu, F., Timofte, R., Van Gool, L.: Repaint: Inpainting using denoising diffusion probabilistic models. In: Proceedings of the IEEE/CVF Conference on Computer Vision and Pattern Recognition. pp. 11461–11471 (2022) [1](#)
26. midjourney: midjourney, <https://www.midjourney.com/>, Last accessed on 2024-02-28 [1](#)
27. Modelscope: face-quality-assessment, [https://modelscope.cn/models/iic/cv\\_manual\\_face\\_quality\\_assessment\\_fqa/summary](https://modelscope.cn/models/iic/cv_manual_face_quality_assessment_fqa/summary), Last accessed on 2024-02-28 [1](#), [2](#), [7](#), [8](#), [10](#)
28. Nichol, A., Dhariwal, P., Ramesh, A., Shyam, P., Mishkin, P., McGrew, B., Sutskever, I., Chen, M.: Glide: Towards photorealistic image generation and editing with text-guided diffusion models. arXiv preprint arXiv:2112.10741 (2021) [1](#), [3](#)
29. Nichol, A.Q., Dhariwal, P.: Improved denoising diffusion probabilistic models. In: International Conference on Machine Learning. pp. 8162–8171. PMLR (2021) [1](#)
30. playgroundai: Mjhg-30k, <https://huggingface.co/datasets/playgroundai/MJHQ-30K>, Last accessed on 2024-02-28 [12](#)
31. Podell, D., English, Z., Lacey, K., Blattmann, A., Dockhorn, T., Müller, J., Penna, J., Rombach, R.: Sdxl: Improving latent diffusion models for high-resolution image synthesis. arXiv preprint arXiv:2307.01952 (2023) [1](#), [2](#), [4](#), [5](#), [10](#)
32. Radford, A., Kim, J.W., Hallacy, C., Ramesh, A., Goh, G., Agarwal, S., Sastry, G., Askell, A., Mishkin, P., Clark, J., et al.: Learning transferable visual models from natural language supervision. In: International conference on machine learning. pp. 8748–8763. PMLR (2021) [4](#), [9](#)
33. Rafailov, R., Sharma, A., Mitchell, E., Ermon, S., Manning, C.D., Finn, C.: Direct preference optimization: Your language model is secretly a reward model. arXiv preprint arXiv:2305.18290 (2023) [4](#)
34. Ramesh, A., Dhariwal, P., Nichol, A., Chu, C., Chen, M.: Hierarchical text-conditional image generation with clip latents. arXiv preprint arXiv:2204.06125 [1\(2\)](#), [3](#) (2022) [1](#), [3](#)
35. Rombach, R., Blattmann, A., Lorenz, D., Esser, P., Ommer, B.: High-resolution image synthesis with latent diffusion models. In: Proceedings of the IEEE/CVF conference on computer vision and pattern recognition. pp. 10684–10695 (2022) [1](#), [2](#), [3](#), [5](#), [8](#), [10](#), [12](#), [13](#), [14](#)

36. Ronneberger, O., Fischer, P., Brox, T.: U-net: Convolutional networks for biomedical image segmentation. In: Medical Image Computing and Computer-Assisted Intervention–MICCAI 2015: 18th International Conference, Munich, Germany, October 5–9, 2015, Proceedings, Part III 18. pp. 234–241. Springer (2015) 4
37. Ruiz, N., Li, Y., Jampani, V., Pritch, Y., Rubinstein, M., Aberman, K.: Dreambooth: Fine tuning text-to-image diffusion models for subject-driven generation. In: Proceedings of the IEEE/CVF Conference on Computer Vision and Pattern Recognition. pp. 22500–22510 (2023) 3
38. Saharia, C., Chan, W., Saxena, S., Li, L., Whang, J., Denton, E.L., Ghasemipour, K., Gontijo Lopes, R., Karagol Ayan, B., Salimans, T., et al.: Photorealistic text-to-image diffusion models with deep language understanding. *Advances in Neural Information Processing Systems* **35**, 36479–36494 (2022) 1, 3
39. Schuhmann, C., Beaumont, R., Vencu, R., Gordon, C., Wightman, R., Cherti, M., Coombes, T., Katta, A., Mullis, C., Wortsman, M., et al.: Laion-5b: An open large-scale dataset for training next generation image-text models. *Advances in Neural Information Processing Systems* **35**, 25278–25294 (2022) 8
40. SG161222: Realistic\_vision\_v5.1, [https://huggingface.co/SG161222/Realistic\\_Vision\\_V5.1\\_noVAE](https://huggingface.co/SG161222/Realistic_Vision_V5.1_noVAE), Last accessed on 2024-02-28 1, 2, 5, 6, 10, 13, 14
41. Shen, X., Du, C., Pang, T., Lin, M., Wong, Y., Kankanhalli, M.: Finetuning text-to-image diffusion models for fairness. arXiv preprint arXiv:2311.07604 (2023) 3
42. Song, J., Meng, C., Ermon, S.: Denoising diffusion implicit models. In: International Conference on Learning Representations (2020) 4, 10
43. Song, Y., Ermon, S.: Generative modeling by estimating gradients of the data distribution. In: *Advances in Neural Information Processing Systems*. pp. 11895–11907 (2019) 4
44. Song, Y., Sohl-Dickstein, J., Kingma, D.P., Kumar, A., Ermon, S., Poole, B.: Score-based generative modeling through stochastic differential equations. In: International Conference on Learning Representations (2020) 1, 4
45. Vaswani, A., Shazeer, N., Parmar, N., Uszkoreit, J., Jones, L., Gomez, A.N., Kaiser, Ł., Polosukhin, I.: Attention is all you need. *Advances in neural information processing systems* **30** (2017) 9
46. Wallace, B., Dang, M., Rafailov, R., Zhou, L., Lou, A., Purushwalkam, S., Ermon, S., Xiong, C., Joty, S., Naik, N.: Diffusion model alignment using direct preference optimization. arXiv preprint arXiv:2311.12908 (2023) 4, 12, 13, 14
47. Wu, X., Sun, K., Zhu, F., Zhao, R., Li, H.: Human preference score: Better aligning text-to-image models with human preference. In: Proceedings of the IEEE/CVF International Conference on Computer Vision. pp. 2096–2105 (2023) 1, 2, 3, 4, 7, 8
48. Xu, J., Liu, X., Wu, Y., Tong, Y., Li, Q., Ding, M., Tang, J., Dong, Y.: Imageward: Learning and evaluating human preferences for text-to-image generation. arXiv preprint arXiv:2304.05977 (2023) 1, 2, 3, 4, 7, 8, 9, 10
49. Zhang, L., Rao, A., Agrawala, M.: Adding conditional control to text-to-image diffusion models. In: Proceedings of the IEEE/CVF International Conference on Computer Vision. pp. 3836–3847 (2023) 3, 4
50. Zhang, Y., Qin, Z., Liu, Y., Campbell, D.: Detecting and restoring non-standard hands in stable diffusion generated images. arXiv preprint arXiv:2312.04236 (2023) 4



**Fig. 9:** More images with faces generated by our fine-tuned model based on RV5.1 and  $\ell_2$  distance measure. We omit the prompts for simplicity and focus on the face quality.

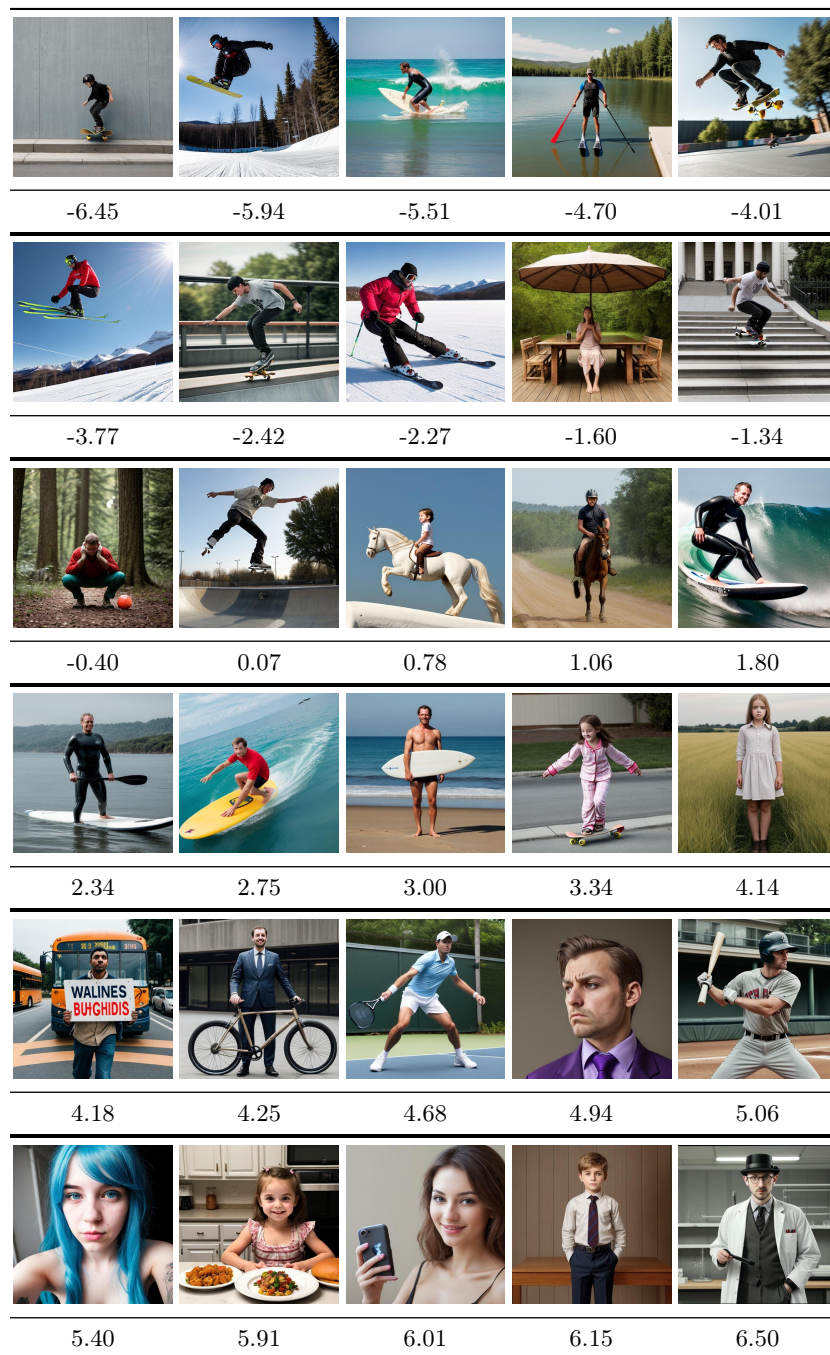


**Fig. 10:** More random face images and the corresponding *Face Score* in increasing order. We can observe a trend that higher scores indicate better quality of facial generation.

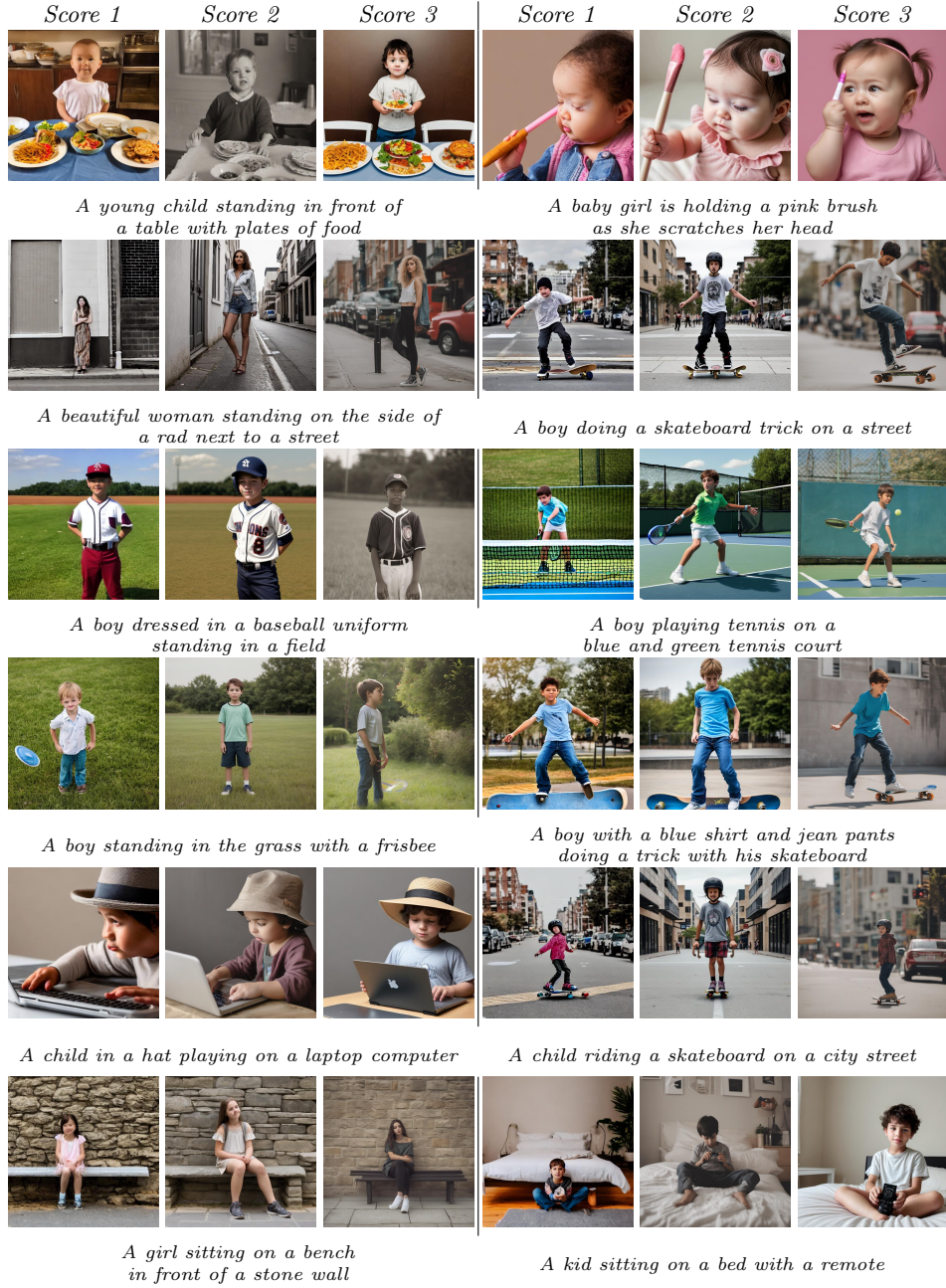


**Fig. 11:** More examples of the human-annotated triplet. The image with higher face quality is assigned a higher score. We can see despite RV5.1 having a smaller model size and fewer model parameters, its facial quality is comparable to that of SDXL.





*children raising their hands in class*



*man in camouflage uniform*



*woman flying on a rocket  
pop art retro vector illustration*



*woman in white shirt and blue pants  
standing in front of a church*



*man doing yoga in front of waterfall*



*man of steel hd wallpaper*



*man of steel trailer*



*woman dancing on the beach*



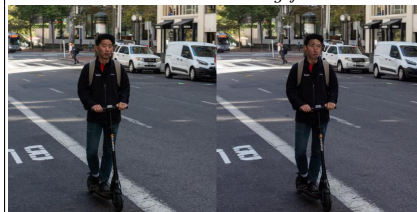
*man on a scooter*



*woman pushing shopping cart  
with Christmas gifts*



*woman with broken car and tire on road*



*man sitting on a scooter*



**Fig. 12:** More examples of face pairs. We leverage the inpainting pipeline and control the noise factor for a degraded version, thereby forming a (good, bad) face pair.